^{51}V NMR study of the kagome staircase compound $Ni_3V_2O_8$

V. Ogloblichev,[1,2] K. Kumagai,[1] S. Verkhovskii,[2] A. Yakubovsky,[3] K. Mikhalev,[2] Yu. Furukawa,[1] A. Gerashenko,[2] A. Smolnikov,[2] S. Barilo,[4] G. Bychkov,[4] and S. Shiryaev[4]

[1]*Department of Physics, Faculty of Science, Hokkaido University, Sapporo 060-0810, Japan*

[2]*Institute of Metal Physics, Ural Division of Russian Academy of Sciences, Ekaterinburg 620041, Russia*

[3]*Russian Research Centre, "Kurchatov Institute," Moscow 123182, Russia*

[4]*Institute of Solid State and Semiconductor Physics, Minsk 220072, Belarus*

(Received 27 January 2010; revised manuscript received 10 March 2010; published 5 April 2010)

We used ^{51}V NMR to study magnetic ordering in the $Ni_3V_2O_8$ single crystal with a Kagome staircase structure of Ni atoms. The NMR spectra were measured in the temperature range $T=(3-300)$ K and magnetic fields $H=(2-9.4)$ T directed along the main $\boldsymbol{a},\boldsymbol{b},\boldsymbol{c}$ axes of the orthorhombic (*Cmca*) crystal. The local magnetic field at the ^{51}V NMR probe determines position and the shape of the corresponding NMR line. These parameters yield an unique information, respectively, on the uniform and the staggered spin components of the ordered Ni. The NMR data collected at $H\geq 2$ T are considered in line with predictions of the representation theory [A. Harris, Phys. Rev. B **76**, 054447 (2007)] with a result that incommensurate amplitude-modulated structure of the spine Ni_s spins acquires in the high-temperature incommensurate (HTI) phase two prominent nearly equal spin components $S_a \approx S_c \gg S_b$ instead of the longitudinal incommensurate spin-density wave (SDW) order with $S_a \gg S_c, S_b$ as it was deduced from neutron-diffraction data [M. Kenzelmann *et al.*, Phys. Rev. B **74**, 014429 (2006)]. No *noticeable* variation of SDW polarization in the ***ab*** plane was detected below the HTI-low-temperature incommensurate (LTI) transition. In both the HTI and LTI phases two almost equal spin components of the Ni_s spins $S_a \approx S_c \gg S_b$ exist at $H<4.7$ T. Their phasing is still not determined. The bulk magnetization in these phases is explained by contribution of the cross-tie Ni_c spins which antiferromagnetic structure in the LTI phase is canted along H.

DOI: 10.1103/PhysRevB.81.144404 PACS number(s): 76.60.−k, 75.40.−s, 75.50.−y

I. INTRODUCTION

Intensively studied triple oxides $Me_3V_2O_8$ (Me=Cu, Ni, Co, and Mn) (Refs. 1–3) represent geometrically frustrated magnets where the triangle Kagome lattice of Me ions can result in diverse energetically degenerate states with different orientations of the neighbor spins. In the orthorhombic *Cmca* structure of the oxides the Kagome staircase lattice appears with partially lifted degeneracy due to evident single-axis crystal anisotropy. Nevertheless, in anisotropic Kagome staircase structure the competition of comparable exchange interactions between magnetic ions manifests itself at low temperature in the consecutive magnetic phase transitions exhibiting new examples of long- and short-range magnetic ordering.

The low-temperature magnetic order in $Ni_3V_2O_8$ is of special interest due to the observation of homogeneous ferroelectric polarization[4] in one of magnetic phases displaying incommensurate modulated spin structure of the Ni spins.[5–8] The $Ni_3V_2O_8$ (NVO) oxide represents magnetic insulator with orthorhombic crystal structure (space group *Cmca* No. 64).[9–11] The structure schematically shown in Fig. 1 consists of two different types of $Ni^{2+}(3d^8,\ S=1)$ ions: Ni_s—"spine" and Ni_c—"cross tie," which form the chains of Kagome staircases along ***a*** axis in the ***ac*** plane. The neighbor staircases are separated by the layers of slightly distorted VO_4 tetrahedrons which stabilize the oxide crystal structure. The nonmagnetic $V^{5+}(3d^0)$ ions occupy structurally equivalent sites surrounded with six Ni_s-(s1-s6) and three Ni_c-(c1-c3) magnetic neighbors[11,12] as shown for V1 atom in Fig. 1.

The material is paramagnetic (PM) above 10 K. Below this temperature the magnetic ordering of Ni^{2+} ions appears

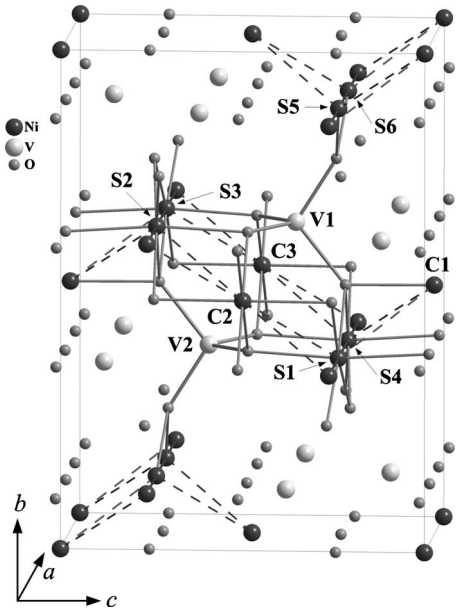

FIG. 1. Schematic nearest-neighboring environment of vanadium (V1) by the "Ni_s—spine" (s1-s6) and "Ni_c—cross-tie" (c1-c3) nickel atoms in the Kagome-staircase orthorhombic structure of $Ni_3V_2O_8$. The dashed lines connecting Ni atoms illuminate the Kagome pattern of the structure. The Ni-O, O-V bonds responsible for the spin-polarization transfer at the nonmagnetic V atoms are shown with gray solid lines.

as follows from the magnetization, heat capacity, and neutron diffraction data.[1,3,5,11] The magnetic order of the high-temperature incommensurate (HTI) dielectric phase is represented with longitudinal spin-density wave (SDW) of the Ni_s spins, predominantly polarized along the ***a*** axis. Whereas entering below 6.4 K to the low-temperature incommensurate (LTI) ferroelectric phase both the Ni_s and Ni_c moments point the cycloid spiral in the ***ab*** plane with the wave vector again along ***a***.[11] In zero magnetic field the phases with commensurate antiferromagnetic order, the high-temperature phase (CAF) and the low-temperature one (C'AF), appear only below 4 K.

The microscopic information coming from the neutron-diffraction experiments performed hand in hand with the comprehensive symmetry consideration is mainly relevant to the staggered magnetic order developed in the incommensurate phases while the uniform magnetic components of nickel remain almost hidden. In this paper we studied the distribution of spin density in paramagnetic and incommensurate magnetic phases of the NVO single crystal by measuring ^{51}V NMR in the temperature range $T=(3-300)$ K at magnetic fields $H=(2-9.4)$ T. It is shown that the ^{51}V NMR line is shifted due to the local magnetic field originating in the spin polarization transferred from the magnetic (Ni_s, Ni_c) neighbors to the nonmagnetic V^{5+} ion. The modulated spin structures varying both the magnitude and direction of local field from one vanadium site to another produce specific NMR line shape. The investigation of magnetic order for the incommensurate HTI and LTI phases which differ by the absence and presence of ferroelectric domain structure, correspondingly,[4] is of the main concern. The ^{51}V NMR data are discussed taking into account the bulk magnetization data measured in the same sample at the same magnetic fields directed along the main crystal axis $\boldsymbol{H}\|\boldsymbol{a}$, $\boldsymbol{H}\|\boldsymbol{b}$, and $\boldsymbol{H}\|\boldsymbol{c}$ to elucidate the features of local ferromagnetic (FM) and antiferromagnetic spin correlations of the nickel ions in the NVO crystal.

II. SAMPLES AND METHODS

Single crystals were grown by spontaneous crystallization from the fluxed melt based on the solvent BaO-V_2O_5. The route of growth has been already used for these vanadates.[3] Under optimized growth conditions $BaCO_3$, NiO, and V_2O_5 powders (all of 99.99% purity) were mixed in molar ratio 1:1:1.5 and placed in a high-density alumina crucible. After a common procedure of the mixture calcination in air at 900 °C and following homogenization of the fluxed melt at 1200 °C during eight hours, temperature in the furnace with vertical heating elements was decreased down to 900 °C at the rate 1 °C/h. Then the rest of the fluxed melt was quickly removed from the crucible and the grown crystals were cooled down to room temperature at a rate of 50 °C/h for about 15 h. The grown crystals of deep dark gray color had a rhombic plate habit with up to 2 cm^2 square surface of the main rhombic face of the {010} type and thickness in the range (1–1.5) mm along ***b*** axis. For the well-shaped single crystals the ***a*** and ***c*** axes coincide well with the rhombic face diagonals. The x-ray fluorescent analysis confirmed desirable cations ratio in the grown crystals as well as the absence of barium within the detection limit level.

The room-temperature lattice parameters of the orthorhombic *Cmca* structure $a=5.931(6)$ Å, $b=11.374(8)$ Å, and $c=8.235(5)$ Å were determined in the x-ray powder-diffraction studies of several samples prepared from crushed single crystals, and this result is in agreement with the published structural data.[11] The low-temperature electric properties, ac permittivity and static electric polarization, of a plate-like crystal taken from the same batch are reported elsewhere.[13] Magnetic susceptibility $\chi=M/H$ was measured with a superconducting quantum interference device magnetometer MPMS-7 (Quantum Design) in the temperature range $T=(2-300)$ K including both heating up and cooling down the sample at magnetic fields $H=(0.01-7)$ T.

NMR spectra of ^{51}V ($^{51}\gamma=\nu_0/H_0=11.193$ MHz/T) were obtained with a conventional spin-echo technique $[\pi/2\text{-}t\text{-}\pi\text{-}t\text{-}E(2t)]$ by field sweep at some fixed frequencies $\nu_0=22.9$; 53.01; and 81.06 MHz of the radio pulses $(\pi/2;\pi)$ exciting echo signal $E(2t)$, as well as by frequency sweep at the fixed magnetic field $H_0=9.4$ T. The shifts of the lines $K=(H_0-H)/H_0$ at the field sweep and $K=(\nu-\nu_0)/\nu_0$ at the frequency sweep were measured relative to the position (H_0/ν_0) of the ^{51}V NMR line in the water solution of KVO_3 taken as a standard reference $(K=0)$.

III. RESULTS AND DISCUSSIONS

A. Paramagnetic phase

Before going to discussion of magnetic properties a summary is presented of local charge symmetry around vanadium ions as it follows from the ^{51}V NMR measurements of the electric field gradient tensor at V sites.

1. Electric field gradient and symmetry of charge environment at the vanadium site

The ^{51}V spectra of the NVO single crystal measured at $H=9.4$ T are shown in Fig. 2. The spectrum consists of two lines with very different intensities. The line of small intensity with a temperature-independent shift $K(T=300\ \text{K})\approx 0$ is assigned to a small amount of V_2O_5—one of the flux components used in the crystal growth. Second line of the dominating intensity with a large shift $[K(T=300\ \text{K})\approx 1.5\%]$, dependent on both temperature and crystal-axes orientation in external magnetic field ***H***, originates from vanadium atoms in the NVO crystal. With variation in the crystal orientation in the field the line shows a structure of $(2I+1)=7$ peaks arising due to an anisotropic interaction of the quadrupolar nuclear moment of ^{51}V ($I=7/2$; $e^{51}Q=0.052\times 10^{-24}$ cm^2) with the electric field gradient (EFG) V_{ii}. It is worth noting that the orientation dependence of the fine structure splitting indicates that our thick NMR crystal consists of some glued thin single-crystal plates misaligned lightly (about 8°) in the ***ac*** plane.

The orientation dependence of NMR line splitting has allowed determining the symmetry and the directions of the principal axes $(OX;OY;OZ)$ of the EFG tensor at V sites. The EFG tensor $\{V_{XX};V_{YY};V_{ZZ}\}$ has an asymmetry parameter

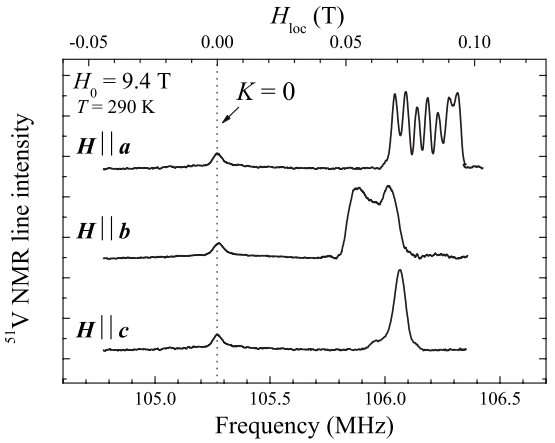

FIG. 2. ^{51}V NMR spectra measured at $T=290$ K in the paramagnetic state of the $Ni_3V_2O_8$ single crystal differently oriented in external magnetic field $H_0=9.4$ T. An additional line of small intensity with magnetic shift nearby $K=0$ (shown by vertical dotted line) originates from a small amount of V_2O_5—one of the flux components used during the crystal growth.

$\eta=(V_{XX}-V_{YY})/V_{ZZ}=0.4(1)$ and the quadrupole frequency $\nu_Q=1/14(e^2QV_{ZZ}/h)=160(15)$ kHz corresponding to the largest value of the line splitting. The main EFG axis ***OZ*** is lying at the ***bc*** plane and has an angle of 54(3)° to the ***c*** axis of the crystal. The ***OX*** axis is directed along ***a***. For such orientation of the main EFG axes the minimal quadrupolar splitting of NMR line is expected in magnetic field along the ***c*** axis, which is in accordance with the line for $\boldsymbol{H}\|\boldsymbol{c}$ in Fig. 2. Thus, at room temperature, the charge distribution around the V site results in the EFG tensor which symmetry reflects strongly the crystal symmetry dictated for that site in the orthorhombic *Cmca* structure.

With temperature decrease the fine quadrupolar structure of the line is masked due to inhomogeneous magnetic broadening which contribution $(\delta H)\propto T^{-1}$ starts to exceed the quadrupole splitting $(\nu_Q/^{51}\gamma)$ below 150 K. If that is the case,[14] the nonselective excitation of the line with the π-pulse width $\tau_\pi<(\nu_Q)^{-1}$ results in modulating behavior of the ^{51}V echo amplitude $E(2t)\propto\exp(-2t/T_2)[1+A\cos(\pi\nu_{beat}t)]$ with the modulation index $|A|<1$. The beat frequency ν_{beat} depends on the crystal orientation in magnetic field, i.e., $\nu_{beat}(\boldsymbol{H}\|\boldsymbol{a})\propto V_{ZZ}$, etc.[14,15] Figure 3 shows an example of the $E(2t)$ vs $(2t)$ beats detected in the NVO crystal at $T=30$ K where inhomogeneous magnetic broadening of the line $(\delta H)\sim 0.05$ T $\gg \nu_Q/^{51}\gamma$. These quadrupolar beats allow monitoring the EFG at vanadium down to the PM-HTI phase transition. It is found that $\nu_{beat}(\boldsymbol{H}\|\boldsymbol{a})$, $\nu_{beat}(\boldsymbol{H}\|\boldsymbol{b})$, and $\nu_{beat}(\boldsymbol{H}\|\boldsymbol{c})$ remain unchanged down to 10 K thus evidencing for invariable local symmetry of the charge environment at vanadium site in the paramagnetic state of NVO.

2. *Magnetic susceptibility and* ^{51}V *NMR line shift*

In PM state magnetic susceptibility follows the Curie-Weiss law $\chi_{a,b,c}=C_{a,b,c}/(T-\Theta_{a,b,c})$ with the Curie constants $C_{a,b,c}=1.22(1)$, 1.26(2), and 1.30(1) emu K/mol at.Ni and the negative Weiss constant values $\Theta_{a,b,c}=-13(2),-16(2),-16(2)$ K for magnetic field directed along ***a***, ***b***, and ***c*** crystal axes, respectively. The obtained mean-field parameters are in consistency with those recently reported for single crystal studied by the neutron diffraction.[11] The linear plots $\chi^{-1}(T)=H/M(T)$ in Fig. 4(a) hold down to the transition into a magnetically ordered state. Insignificant anisotropy of χ in the PM state is indicative that spin magnetism of nickel, χ_s, dominates over other contributions, and the nickel ions are in the orbital singlet state with strongly suppressed orbital magnetism.[9] Indeed, an estimate of the effective magnetic moment $\mu_{\mathrm{eff},a,b,c}=3.1(3),3.2(4),3.2(4)\mu_B$ per Ni is only slightly higher than $\mu_{\mathrm{eff}}=2.83\mu_B$ of the $Ni^{2+}(3d^8;\ S=1)$ ion in the cubic crystal field.

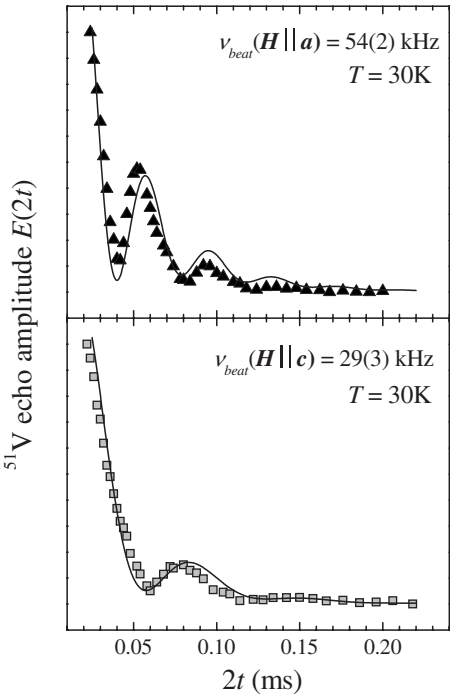

FIG. 3. The ^{51}V echo amplitude $E(2t)$ versus $2t$, the double time delay between radio pulses forming echo signal, in the $Ni_3V_2O_8$ single crystal at $T=30$ K and different orientations of the ***a*** and ***c*** axes with respect to magnetic field direction H. Solid lines are the fit with an expression $E(2t)\propto\exp(-2t/T_2)[1+A\cos(\pi\nu_{beat}t)]$.

The ^{51}V NMR line shift $K_{a,b,c}$ measured at $\boldsymbol{H}\|\boldsymbol{a}$, $\boldsymbol{H}\|\boldsymbol{b}$, and $\boldsymbol{H}\|\boldsymbol{c}$ takes the positive value in the whole temperature range of the PM phase. Its temperature dependence can be well described with an expression $K_{a,b,c}(T)=K_{0,a,b,c}+C_{a,b,c}/(T-\Theta_{a,b,c})$ including the Curie-Weiss term where the Weiss constants $\Theta_{\mathrm{NMR},a,b,c}=-15(2),-7(3),-6(3)$ K are again negative. The temperature independent term K_0 is determined by the orbital and diamagnetic contributions of electrons in the filled valence shells. Below 300 K its value is negligible as compared with the total shift. It is well seen from Fig. 4(b) where the $(K_{a,b,c})^{-1}$ data plotted vs T are reasonably approximated by linear fits. The strong inequality $K_0\ll K_{a,b,c}(T)$ presumes an empty d shell in the electron configuration of transition-metal ion, as it was suggested for the vanadium ions in NVO.[1,9]

Figure 4(c) shows the parametric dependence of the line shift on magnetic susceptibility with temperature as a parameter. In paramagnetic phase the $K_{a,b,c}(\chi_{a,b,c})$ plots can be well

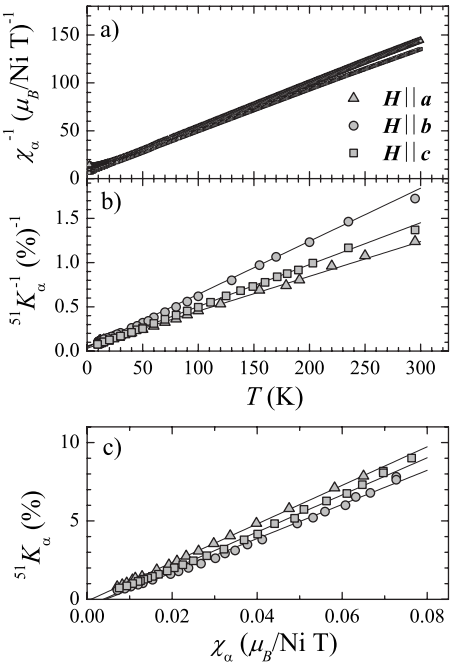

FIG. 4. Temperature dependence of the inverse magnetic susceptibility $\chi_{a,b,c}-(a)$, the inverse ^{51}V NMR line shift $K_{a,b,c}-(b)$, and the parametric $K_{a,b,c}$ versus $\chi_{a,b,c}$ dependence—(c) in the paramagnetic state of the $Ni_3V_2O_8$ single crystal differently oriented in magnetic field: (△)—$\boldsymbol{H}\|\boldsymbol{a}$, (○)—$\boldsymbol{H}\|\boldsymbol{b}$, and (□)—$\boldsymbol{H}\|\boldsymbol{c}$. The straight lines are the corresponding fits (see the text).

approximated by linear dependencies which visually evidence that the large positive NMR shift at nonmagnetic vanadium is completely controlled by spin magnetism of Ni_s and Ni_c ions. A slope of the fitting lines defines the local field $H_{loc}=(K/\chi_{mol})\mu_B 3N_A$ created at the vanadium by magnetic moment in $1\mu_B$ of the nickel neighbors: $H_{loc,a}=1.23$ T/μ_B, $H_{loc,b}=1.01$ T/μ_B, and $H_{loc,c}=1.18$ T/μ_B.

The large value of H_{loc} displays remarkably slight change at different orientation of the crystal in the applied field. Estimation of the classic dipolar field created at V by nine nearest Ni ions, each having the static magnetic moment $g_e\mu_B\langle S_z(Ni^{2+};\mu_{eff}\approx 3\mu_B)\rangle=\chi_s H$ along $\boldsymbol{H}$, results in the inequality

$$H_{dip}=\frac{\chi_s H}{(r_{Ni\text{-}V})^3}\left|\sum_{i=1}^{9}[3\cos^2(\widehat{\boldsymbol{Hr}}_{(Ni\text{-}V)i})-1]\right| \approx (0.05-0.07)T \ll H_{loc}. \quad (1)$$

Thus the dipolar interaction can be responsible only for small anisotropy of H_{loc} but does not explain its noticeably large positive value.[16]

Among isotropic hyperfine magnetic interactions the most probable one is the Fermi contact interaction of the nuclear spin ^{51}I with the transferred s-spin density of electrons participating both in the Ni-O-Ni bonding and in superexchange coupling of the neighboring $6Ni_s$ and $3Ni_c$. It is worth noting that the corresponding local field $\boldsymbol{h}$ created by transferred spin density $f\langle\boldsymbol{S}(Ni)\rangle$ of *one* of the Ni neighbors

$$\boldsymbol{h}=H_{FC}(4s)f\mu_{eff}(Ni)/\mu_B=H_{FC}(4s)f\langle\boldsymbol{S}(Ni)\rangle \quad (2)$$

is collinear to the $\langle\boldsymbol{S}(Ni)\rangle$, the thermal averaged electron spin of Ni.

$$\boldsymbol{H}_{loc}=\sum_i \boldsymbol{h}_i=H_{FC}(4s)\sum_i f_i\langle\boldsymbol{S}(Ni_i)\rangle. \quad (3)$$

Here $H_{FC}(4s)=110$ T is the corresponding isotropic hyperfine magnetic field due to the Fermi-contact interaction with an electron at the $4s$ orbital.[17] The spin density transferred at vanadium from neighboring Ni ions is defined in terms of the factor $f_i=h_i/2H_{FC}(4s)$.[18] This quantity estimated from Eq. (3) results in $f<0.002$, the effective fractional occupancy of the $4s$(V) orbital by the unpaired electron of Ni.

According to Eq. (3) the value and direction of H_{loc} are determined by the vector sum of $\boldsymbol{h}_i\uparrow\uparrow\langle\boldsymbol{S}(Ni_i)\rangle$ which is sensitive to static spin correlations of the nearest magnetic ions. In the PM state far from the magnetic transition only the component $h_z\propto\langle S_z(Ni)\rangle$ along magnetic field $\boldsymbol{H}\|\boldsymbol{z}$ remains static both for Ni_s and Ni_c spins. The estimated average $\langle h_a\rangle=1/9(K_a/\chi_{mol})\mu_B 3N_A=0.138(10)$ T/μ_B per one Ni neighbor is calculated under the assumption of equal absolute values of local fields created at ^{51}V by the Ni_s and Ni_c neighbors. In fact, they have distinct pathways for the transferred spin polarization and contribute variously to the shift and the width of ^{51}V NMR line in the magnetic phases exhibiting staggered spin order. This difference will be specified in the separate estimate of h_s for Ni_s and h_c for Ni_c [see Eqs. (5) and (6)].

The NMR line shape remains unchanged below 70 K. Only its width is gradually increased due to magnetic contributions exceeding considerably the one from electric quadrupole interaction. The representative spectra acquired at $T=15$ K and different orientations of the crystal in magnetic field are shown at the upper panels (a) and (b) of Fig. 5. For simplicity of comparison, an intensity of the lines is plotted against $H_{loc}=H_0-H$. An asymmetry of the line at $\boldsymbol{H}\|\boldsymbol{a}$ and its double-peak shape at $\boldsymbol{H}\|\boldsymbol{c}$ is a consequence of the insignificant misalignment in $\boldsymbol{ac}$ plane of the single crystal plates forming the bulk NMR crystal. This additional broadening was taken into account in the analysis of the specific NMR line shapes emerging in magnetically ordered state of the NVO crystal. The typical multipeak lines summarized in Fig. 5 reflect staggered ordering of the Ni spins in the HTI and LTI phases.

B. Magnetically ordered state

The magnetization isotherms $M(H;T=\text{const})$ measured along the main crystal axes are shown in Fig. 6 at some temperatures corresponding to the different types of magnetic order. In both $M(H;T=\text{const})$ and M $(T;H=\text{const}$; not shown) magnetization dependencies consistent with the well known $(T;H)$-magnetic phase diagram of NVO crystal at ($\boldsymbol{H}\|\boldsymbol{a}$, $\boldsymbol{H}\|\boldsymbol{b}$, and $\boldsymbol{H}\|\boldsymbol{c}$) are observed.[3,11] Further this phase diagram is used to compare static magnetic order following from the ^{51}V NMR data obtained in $H=2$, 4.7, and 7 T with the corresponding (H,T)—areas of the different phases.

The single NMR line sharply broadens below $T_{HTI}=9.4(4)$ K. With further decreasing T the NMR spectrum

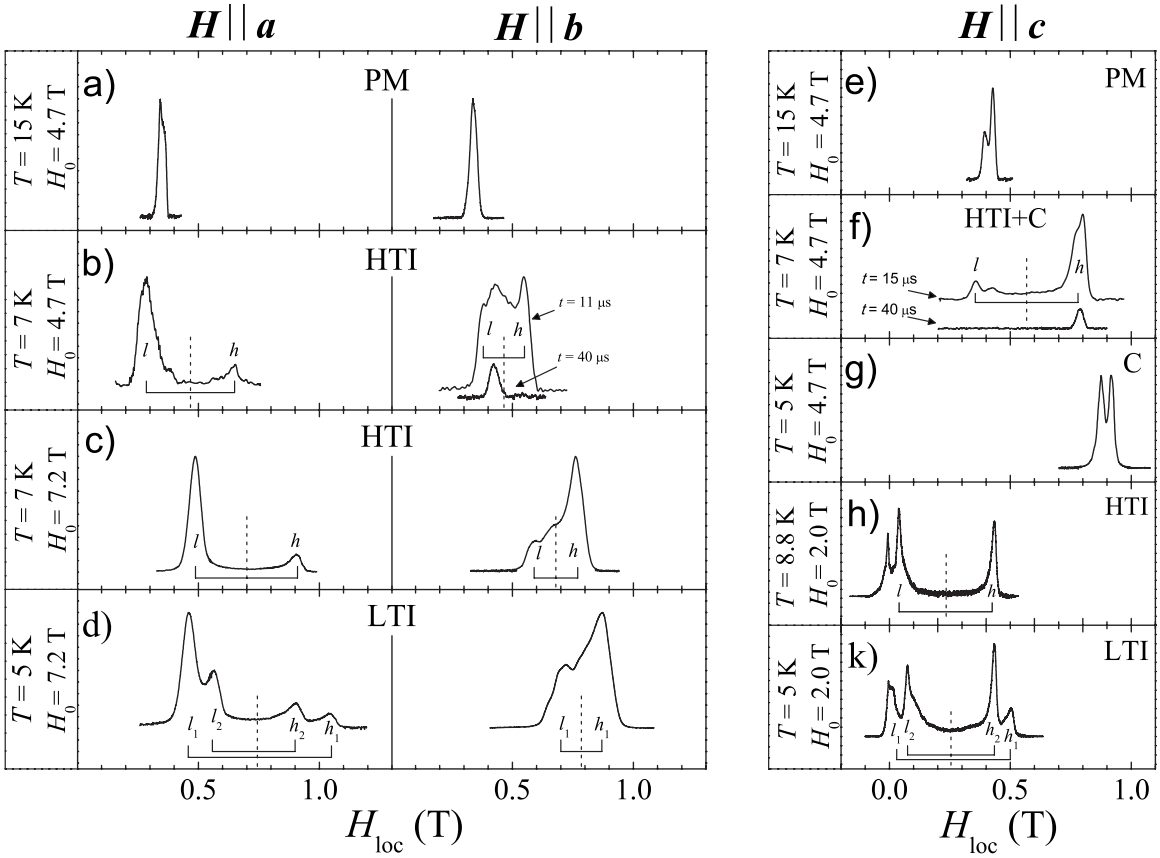

FIG. 5. ^{51}V NMR spectra measured in the $Ni_3V_2O_8$ single crystal at different orientations of the ***a***, ***b***, and ***c*** axes with respect to magnetic field direction ***H*** in (a), (e)—paramagnetic phase, [(b), (c), (f), and (h)]—HTI phase, [(d) and (k)]—LTI phase, and (g)—canted antiferromagnetic (c) phase. The spectra were measured using spin-echo technique (see details in the text) and some of them are labeled with t, the time delay between pulses forming the ^{51}V echo signal.

consisting of several peaks is formed. The typical field-sweep ^{51}V NMR spectra acquired at some fixed frequencies $\nu_0=\gamma H_0$ and $\boldsymbol{H}\|\boldsymbol{a}$, $\boldsymbol{H}\|\boldsymbol{b}$, and $\boldsymbol{H}\|\boldsymbol{c}$ are shown in Fig. 5. The temperature dependence of $H_{\rm loc}$ corresponding to the peaks [labeled as h and l at Figs. 5(b) and 5(c)] is presented in Fig. 7.

Additionally, the ^{51}V echo-decay curve, $E(2t)$, was measured at each of the peaks of the complex spectrum. It is well known[19] that in magnetic insulators the rate of echo decay, T_2^{-1}, at nonmagnetic atoms (like V in NVO) is mediated by low-frequency spin dynamic of magnetic ions. The coincidence of the T_2^{-1} values was used as a criterion for assignment of the peaks in question to vanadium placed in the domains of the same magnetic phase.

1. HTI phase

a. $\boldsymbol{H}\|\boldsymbol{a}$. Let us consider the spectra measured for $\boldsymbol{H}\|\boldsymbol{a}$ at T=7 K [Figs. 5(b) and 5(c)]. The spectrum consists of a single line characterized by a double-peak (l,h) shape with a continuum of nonzero intensity between the peaks. The central position of the double-peak lines [the vertical dotted lines in Figs. 5(b) and 5(c)], $H_{\rm loc,FM}\equiv(H_{{\rm loc},h}+H_{{\rm loc},l})/2$ is shifted proportionally to H while the splitting $\Delta H_a=H_{{\rm loc},h}-H_{{\rm loc},l}$ is almost independent of H. This line shape is typical of incommensurate modulated spin structures.[20] Thus, the two-peak distribution of the local field $H_{{\rm loc},a}$ at nonmagnetic vanadium reflects the static incommensurate modulation of the Ni spins observed early by neutron diffraction along ***a*** at the wave vector $\{q,0,0\}$.[11]

The plane SDW, $S_a({\rm r})=S_a\cos(\boldsymbol{qr}+\varphi_0)$, should results in the edge peaks l and h of equal intensity. The observed asymmetry of the double-peak shape of the line is indicative of an admixture of the higher harmonics to the basic SDW mode. An appearance of higher harmonics can be qualitatively understood within the model with an expression for the free energy of the NVO magnetic system[11] including besides the main contribution of concurrent exchange interactions of the nearest-neighbor $(k=1)$ and next-nearest-neighbor $(k=2)$ Ni_s spins proportionality $S_a(r)S_a(r\pm ka)$ also the quadratic single-ion anisotropy term $S_a(r)^2$. Then the corresponding component of local field $h_{\rm a}(r)$ acquires both the linear $S_a(r)$ and quadratic $S_a(r)^2$ terms

$$h_a=h_{{\rm FM},a}+h_{1,a}\cos(\boldsymbol{qr})+h_{2,a}\cos^2(\boldsymbol{qr}), \qquad (4)$$

where $h_{\rm FM}$ is the component due to the uniform $(q=0)$ FM polarization of the spin system along external magnetic field; h_1 and h_2 are the components dependent on the particular staggered order. In fact, such a nonlinearity demands to describe the HTI phase structure in terms of the soliton lattice

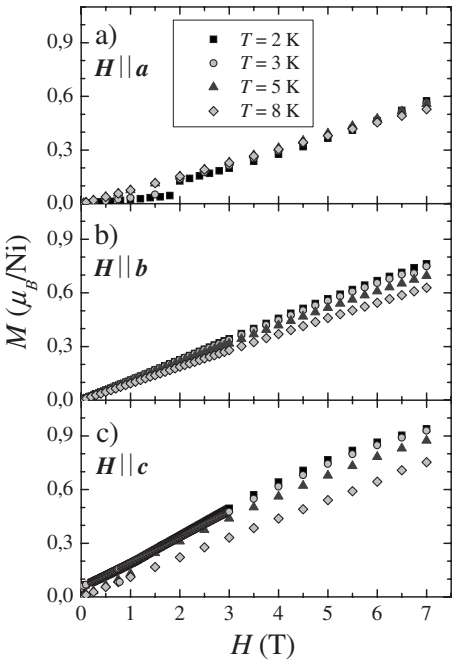

FIG. 6. Magnetization M versus H along the $\boldsymbol{a},\boldsymbol{b},\boldsymbol{c}$ crystal axes of the $Ni_3V_2O_8$ for several temperatures.

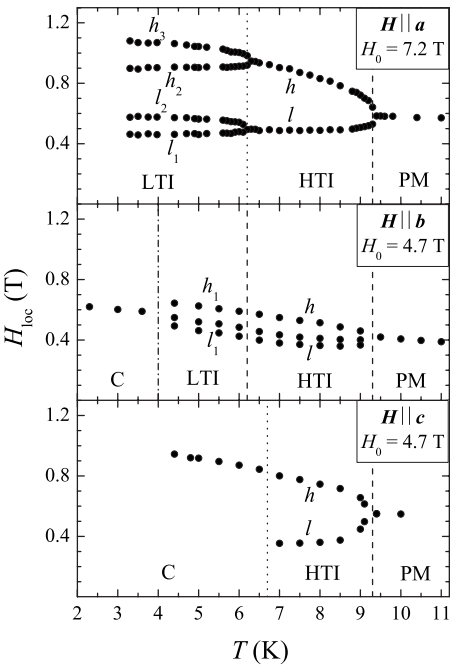

FIG. 7. Low-temperature dependence of the local field $H_{\rm loc}$ corresponding to the positions of the (l,h) peaks of the ^{51}V NMR spectra shown in Fig. 5. The boundaries between phases with different magnetic order are shown by the vertical dotted lines.

with coexisting domains of the commensurate and incommensurate magnetic order.[20] This more sophisticated consideration is beyond the scope of this paper, where we discuss the NMR results within the very same harmonic approximation as it was done in the neutron-diffraction study.[7,11]

The uniform and staggered components of the local field and the corresponding components of magnetization are estimated taking into account the data on $M_a(H,T=8\ \mathrm{K})$ isotherm plotted in Fig. 6(a). Both quantities $H_{\rm loc,FM}(\boldsymbol{H}\|\boldsymbol{a})$ and $M_a(H)$ are positive and increase proportionally to H. In the HTI phase the uniform spin polarization is evidently controlled by Ni_c spins, which are still in disordered PM state due to mutual cancellation of the exchange interactions with the ordered Ni_c neighbors.[11] The local field created at the ^{51}V nuclei by one Ni_c neighbor with $m_c=1\mu_B$ is estimated as

$$h_{\rm c}=1/3H_{\rm loc,FM}(\boldsymbol{H}\|\boldsymbol{a})=0.16(1)\ \ \mathrm{T}/\mu_B \qquad (5)$$

and, correspondingly, from one Ni_s ion

$$h_{\rm s}=1/6\{H_{{\rm loc},a}-H_{\rm loc,FM}(\boldsymbol{H}\|\boldsymbol{a})\}=0.125(10)\ \ \mathrm{T}/\mu_B, \qquad (6)$$

where $H_{{\rm loc},a}=1.23\ \ \mathrm{T}/\mu_B$ is the total local field as it follows from the $K_a(\chi_a)$ plot for the PM phase.

In the ordered phase the local field component along the $\boldsymbol{a}$ axis is modified. Now the vector sum in Eq. (3) depends on the relative phase of SDW components, $m_{{\rm s},a}$, at the neighboring Ni_s chains. It was compelled[6,7,11] that the inversely symmetric dielectric HTI phase adopts only a restricted number of the possible spin structures for NVO. The numerous set of magnetic Brag reflections was described well within the structure where spin components of Ni_s transform according to the irreducible representation Γ^4 of the little group G_q for the incommensurate SDW mode with wave vector $\{q,0,0\}$. The Γ^4 symmetry dictates the following phase relations for amplitude of the $\boldsymbol{a}$ component of Ni_s moments: $m_{s2,a}=-m_{s1,a}=m_{s5,a}$ for $Ni_{s2,s1,s5}$ from adjacent chains and placed in the same $\boldsymbol{bc}$ plane, and $m_{s2,a}=-m_{s3,a}$; $m_{s1,a}=-m_{s4,a}$; and $m_{s5,a}=-m_{s6,a}$ for the neighboring Ni_s ions in the same chain. As a result the local fields at the V1 atom from the (Ni_{s1}-Ni_{s4}) and (Ni_{s5}-Ni_{s6}) chains cancels each other, and the modulated component of $H_{{\rm loc},a}$ is determined explicitly by spin polarization transferred from (Ni_{s2}-Ni_{s3}) chain

$$\begin{aligned}H_{{\rm loc},a}(x)&=h_{\rm s}\{\cos(qx)-\cos[q(x+0.5a)]\}\\&=2h_{\rm s}\sin(qa/4)\sin[q(x+0.25a)].\end{aligned} \qquad (7)$$

The static SDW ($q=2\pi/\lambda$) translated along $\boldsymbol{a}$ creates the double-peak NMR line with the distance between these peaks $\Delta H_a=2\max|H_{1,a}(x)|$. From Eqs. (6) and (7), taking $\lambda=1.73a$,[3] an amplitude of the modulated spin component of Ni_s is estimated as $m_{{\rm s},a}(s2,T=7\ \mathrm{K})=1.8(2)\mu_B$, which is consistent with $m_{\rm s,}=1.9(2)\mu_B$ deduced from the neutron data.[11]

b. $\boldsymbol{H}\|\boldsymbol{c}$. The representative spectra ($\boldsymbol{H}\|\boldsymbol{c}$) obtained at different magnetic fields in the HTI phase are shown in Figs. 5(f)–5(h). The spectrum in Fig. 5(h) obtained at $H=2$ T and $T=9\ \mathrm{K}<T_{\rm HTI}$ is represented by the nearly symmetric double peaked (h,l) line. Such shape of the line indicates clearly the almost harmonic modulated component of local field emerging at the vanadium sites due to the incommensurate SDW component along $\boldsymbol{c}$ axis

$$H_{\mathrm{loc},c}(z) = h_s \cos(qz + \varphi_c) + \cos[q(z + 0.5a) + \varphi_c]$$
$$= 2h_s \cos(qa/4)\cos[q(x + 0.25a) + \varphi_c]. \quad (8)$$

The "+" sign in Eq. (8) is taken in accordance with to the phase relation of the Γ^4 irreducible representation for the spin components along ***c*** axis:[6,7,11] $m_s(s1-s4)=m_{s,c}$, and φ_c is the phase shift of the $m_{s,c}$ component with respect to $m_{s,a}$. An amplitude of the staggered moment $m_{s,c}(T=7\ \mathrm{K}) = 1.9(2)\mu_B$ was estimated in the same way as it is described for $m_{s,a}$ in Sec. I.

The spectrum presented in Fig. 5(f) is obtained at the higher magnetic field of 4.7 T. Its asymmetric spectral pattern depends on t, the time delay between pulses forming the ^{51}V echo signal. With increasing t the spectrum transforms at $t=45\ \mu$s into a single peaked line-2 ($t=45\ \mu$s) while spectral components of another double-peak line-1 presented in the spectrum ($t=10\ \mu$s) vanish due to their fast echo-decay rate. Thus near an upper H boundary of the HTI phase the NVO crystal is represented with two kind of coexisting domains displaying the rich (line-1) and poor (line-2) low-frequency dynamic of the Ni spins. The line-1 holds the same symmetric shape with the splitting $\Delta H_c(H=4.7\ \mathrm{T};T) \approx H_c(H=2\ \mathrm{T};T)$ independent of magnetic field and its shift $H_{\mathrm{loc,FM}} \equiv (H_{\mathrm{loc},h}+H_{\mathrm{loc},l})/2$ increases proportionally to H. The line-1 is evidently originated from the HTI-phase domains. The line-2 can be attributed to domains of the emergent C-phase, which volume fraction grows with further increasing magnetic field.

c. ***H***$\|$***b*** . The spectra for (***H***$\|$***b***) obtained in different magnetic fields at 7 K are shown at the right panel of Figs. 5(b) and 5(c). The spectra consist of two lines which integrate intensities are in ratio 9:1. The lines are easy separated in the spectra acquired with different t. The single peaked line of much less intensity is clearly seen in the spectrum obtained with $t=40\ \mu$s as shown in Fig. 5(b). The origin of this line still cannot be attributed to any of the FM-canted commensurate magnetic structures listed at the (H-T) diagram of NVO.[3]

The line of dominating intensity is splitted in two (h,l) peaks with $\Delta H_b = H_{\mathrm{loc},h} - H_{\mathrm{loc},l}$ being almost independent on H. The line displays fast decay of the echo signal. This line is assigned to vanadium in the HTI-phase domains. At 7 K the splitting ΔH_b is more than twice less of the corresponding $\Delta H_{a,c}$ splittings. Its value of 1.8(2) kOe becomes comparable with the contribution of dipolar fields created along ***b*** by $m_{s,a}$ and $m_{s,b}$ components of Ni$_s$ spins. Taking into account the dipolar corrections an amplitude of the modulated component is estimated as $m_{s,b}(T=7\ \mathrm{K}) = 0.50(20)\mu_B$. That is more than twice $m_{s,b}=0.2(2)\mu_B$ deduced from the neutron data in $H=0$.[11]

Thus, the NMR results presented in this section imply the modulated structure of Ni$_s$ spins acquiring in the HTI phase *two* nearly equal components $S_a \approx S_c \gg S_b$ instead of the longitudinal incommensurate SDW order with $S_a \gg S_c, S_b$ as it was deduced from the neutron diffraction data.[11] The phase shift between the $m_{s,a}$ and $m_{s,c}$ components was determined

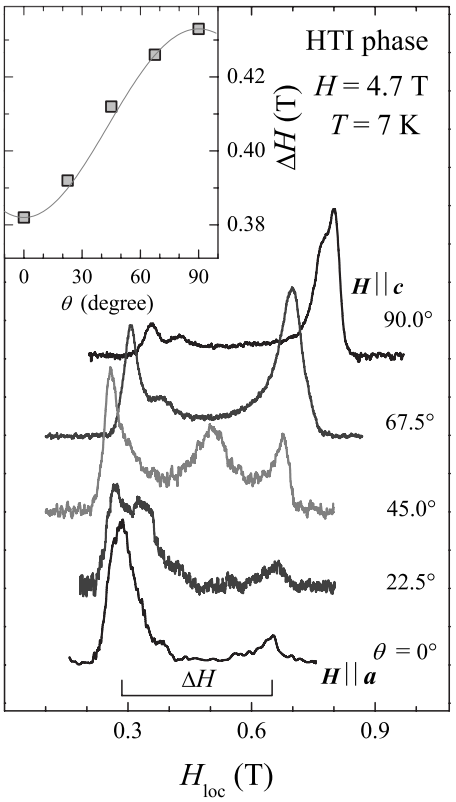

FIG. 8. ^{51}V NMR spectra measured in the HTI phase ($T=7$ K) at ***H***$\|$***ac*** plane and different θ the angle between magnetic field direction and the ***a*** axis of the $Ni_3V_2O_8$ crystal. Inset shows the line splitting data $\Delta H_{ac}(\theta)$ with corresponding fit (solid curve) $\Delta H_{ac}(\theta) = \mathrm{sqrt}(\Delta H_a \cos\theta)^2 + (\Delta H_c \sin\theta)^2$ as explained in the text.

by measuring the angle-dependent splitting $\Delta H_{ac}(\theta)$ of the double-peak line in the spectra shown in Fig. 8. The spectra were obtained at ***H***$\|$***ac*** plane and different θ, the angle between the magnetic field direction and the ***a*** crystal axis. An additional peak appearing in the spectra at $\theta > 0$ is attributed to the *C*-phase domains. With the θ increase the peak is intensified and moves toward the higher H_{loc}. At ***H***$\|$***c*** the peak merges with the double-peak line as shown in the Fig. 5(f). Their separation was described in the previous Sec. III B 1 b. An inset to Fig. 8 shows that the splitting of the double-peak line ΔH_{ac} increases gradually with θ following the dependence $\Delta H_{ac}(\theta) = \mathrm{sqrt}\{(\Delta H_a \cos\theta)^2 + (\Delta H_c \sin\theta)^2\}$ predicted by Eqs. (7) and (8) with $\varphi=0$. This phase relation corresponds to the amplitude-modulated SDW with ***q***$\|$***a*** (according to the neutron data) and the linear polarization nearly along bisector of the $\widehat{ac}$ angle in the ***ac*** plane. This conclusion following from the NMR data is remarkably consistent with the argument that magnetic structure of the dielectric HTI phase should retain an inversion symmetry.[6,7] The HTI magnetic order can be described with two order parameters $m_{s,a}$ and $m_{s,c}$, having the same or opposite phase.

The temperature dependence of the splitting $\Delta H_\alpha \propto m_\alpha (\alpha = a,c)$ as a function of $(T_{\mathrm{HTI}}-T)$ plotted in the double-logarithmic scale at Fig. 9 is well fitted by straight lines with a slope obeying the power dependence $\propto (T_{\mathrm{HTI}}-T)^\beta$ with $\beta_a = 0.37(2)$, $\beta_c = 0.32(4)$, and $T_{\mathrm{HTI}} = 9.3(2)$ K. It is worth

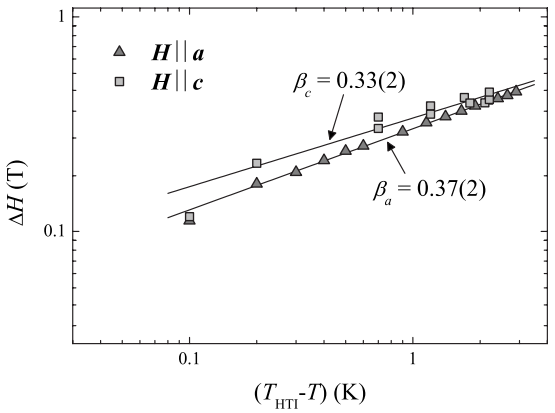

FIG. 9. Temperature dependence of the splitting $\Delta H_\alpha(\alpha=a,c)$ as a function of $(T_{\mathrm{HTI}}-T)$ in the HTI phase of the $Ni_3V_2O_8$ single crystal. The straight lines are the data fits $\propto(T_{\mathrm{HTI}}-T)^{\beta}$ where $\beta_a=0.37(2)$, $\beta_c=0.32(4)$, and $T_{\mathrm{HTI}}=9.3(2)$ K.

noting that estimated values of critical parameters are close to $\beta(n=2)=0.35$ predicted in the Heisenberg isotropic exchange XY model, where the SDW behavior is defined by two order parameters: amplitude and phase. The uniform $H_{\mathrm{loc,FM}}$ component achieves its maximum value at $\boldsymbol{H}$ directed along the $\boldsymbol{c}$ axis. That is accordance with the greatest slope of the $M_c(H;T=\mathrm{const})$ isotherms shown in Fig. 6(c). The nearly isotropic uniform $(q=0)$ polarization of Ni_c spins revealed in the NMR spectra is completely consistent with the neutron data in that the Ni spins remain in the disordered PM state that saves the inverse-symmetric spin structure of the dielectric HTI phase.

2. LTI phase

An additional complication of the NMR spectra below $T_{\mathrm{LTI}}=6$ K indicates on the subsequent symmetry reduction in the ^{51}V spin environment in the LTI phase. The most resolved fine structure of the spectra is obtained at $\boldsymbol{H}\|\boldsymbol{a}$ [Fig. 5(d)] and $\boldsymbol{H}\|\boldsymbol{c}$ [Fig. 5(k)]. Each of the spectra represents a superposition of two lines—doublets (l_1,h_1) and (l_2,h_2) of the corresponding lines (l,h) in the HTI phase. The centers of the doublets are shifted by the same local field $H_{\mathrm{loc,FM}}\propto H_0$ and the doublets have different splitting $\Delta H(l_1,h_1)>\Delta H(l_2,h_2)$ independent of magnetic field in the range of $H=(2-8)$ T for $\boldsymbol{H}\|\boldsymbol{a}$ and $H=(2-4.7)$ T for $\boldsymbol{H}\|\boldsymbol{c}$. The difference $[\Delta H(l_1,h_1)-\Delta H(l_2,h_2)]$ increases with lowering temperature as shown in Fig. 7.

It is easy to understand a specific two-doublet NMR spectra pattern by taking into account that below T_{LTI} the modified incommensurate SDW order involves the modulated components of Ni_c spins with the same wave vector q as for the Ni_s spin system.[11] In fact, spin ordering in the Ni_c sublattice breaks magnetic equivalence of the vanadium ions at the positions above (V1) and under (V2) Kagome staircase which fragment is shown in Fig. 1 with the ions notation.

Let us consider the difference in the magnetic components probed by the V1 and V2 ions for $\boldsymbol{H}\|\boldsymbol{a}$. The V1 ion probes magnetic components $m_{\mathrm{s2},a}$ and $m_{\mathrm{s3},a}$ of Ni_s from the (s2-s3) chain. They are modulated in antiphase with the corresponding components of Ni_s from adjacent (s1-s4) chain $m_{\mathrm{s1},a}=-m_{\mathrm{s2},a}$ and $m_{s4,a}=-m_{\mathrm{s3},a}$, probed by the ion V2. While the modulated $\boldsymbol{a}$ component $H_{\mathrm{c},a}$ of local field coming from $Ni_{\mathrm{c1\text{-}c3}}$ neighbors has the same value and sign at both vanadium sites in question. The value of local field depends on the relative phases $\varphi_{\mathrm{c1\text{-}c3}}$ of the modulated spin components $S_{\mathrm{c},a}$ in the corresponding c1, c2, and c3 Ni_c chains as

$$H_{\mathrm{c},a}(x)=h_c\{\cos(qx+\varphi_{\mathrm{c1}})+\cos[q(x+a)+\varphi_{\mathrm{c2}}]+\cos[q(x+0.5a)+\varphi_{\mathrm{c3}}]\}. \quad (9)$$

The difference in splitting of two doublets

$$[\Delta H(l_1,h_1)-\Delta H(l_2,h_2)]=2h_c\ \max|H_{\mathrm{c},a}(x)| \quad (10)$$

is determined by $2\cdot\max|H_{\mathrm{c},a}(x)|$ by translating static SDW along $\boldsymbol{a}$. The average value $[\Delta H(l_1,h_1)+\Delta H(l_2,h_2)]/2$ is controlled by SDW component $m_{\mathrm{s},a}$ of the Ni_s spins in accordance with Eq. (7).

The very same consideration of the line splitting applied to other orientations of the crystal leads to the following amplitude of SDW components of Ni_s at $T=5$ K:

$$m_{\mathrm{s},a}=1.9(2)\mu_B;\quad m_{\mathrm{s},b}=0.4(2)\mu_B;\quad m_{\mathrm{s},c}=1.8(2)\mu_B. \quad (11)$$

In case of $\boldsymbol{H}\|\boldsymbol{a}$ the spectrum resolution decreases and one can just declare that at the HTI-LTI transition the component $m_{\mathrm{s},b}$ of Ni_s remains unchanged in our accuracy. As a result, in the field range $H=(2-8)$ T NMR probes for LTI phase *no noticeable* variation in SDW polarization in the ***ab*** plane. In both the HTI and the LTI phases two spin components of Ni_s spins are revealed in NMR spectra. At the moment, the collected NMR data do not allow to pickup the relative phasing of these spin components to characterize properly polarization of the SDW emergent in the LTI phase.

Let us turn back to a specific order of the Ni_c spins as it is follows from NMR and magnetization data measured in the LTI phase. According to NMR, the spin system acquires both the uniform $m_{\mathrm{c,FM}}$ and the modulated components. It is interesting that at all H the estimated value of $m_{\mathrm{c,FM}}(H,T=5\ \mathrm{K})=1/3(H_{\mathrm{loc,FM}}/h_c)$ is in the quantitative agreement with the $M(H,T=5\ \mathrm{K})$ data shown in Fig. 6. The bulk magnetization of NVO is reasonably explained by the uniform polarization of the Ni_c antiferromagnetic structure canted along the applied magnetic field H. As shown in Fig. 5(g), at the orientation $\boldsymbol{H}\|\boldsymbol{c}$ the complicated "incommensurate" spectral pattern of the LTI phase shrinks at $H=4.7$ T into a single line shifted to the high H_{loc} values.

IV. CONCLUSION

The magnetic order of Ni spins in different magnetic phases of the $Ni_3V_2O_8$ single crystal was studied by ^{51}V NMR at magnetic fields $H=(2-9.4)$ T directed along the $\boldsymbol{a},\boldsymbol{b},\boldsymbol{c}$ crystal axes. It is shown that both ^{51}V NMR line shift and the line width are very sensitive to specific static spin configuration of the Ni neighbors. These NMR parameters trace, respectively, the uniform $(q=0)$ and the staggered spin components in the magnetic-phases emergent of the NVO crystal at low temperatures. Our main physical conclusions

are listed below: (a) an observation of the double-peak line shape in the ^{51}V NMR spectra below 9 K confirms the incommensurate modulated spin structure existing in both the HTI and the LTI phases. (b) The quantitative analysis of the NMR line splitting made in line with predictions of the representation theory[6,7] shows that incommensurate modulated structure of Ni_s spins acquires in the HTI phase *two* nearly equal spin components $S_a \approx S_c \gg S_b$ instead of the longitudinal incommensurate SDW order with $S_a \gg S_c, S_b$ as it was deduced from the neutron diffraction data.[11] As follows from the NMR data the phase shift between these two spin components corresponds to the amplitude-modulated SDW with $\boldsymbol{q} \| \boldsymbol{a}$ (according to the neutron data) and linearly polarized in $\boldsymbol{ac}$ plane nearly along bisector of the $\boldsymbol{a}\hat{}\boldsymbol{c}$ angle. (c) On going through the HTI-LTI transition no noticeable variation in SDW polarization in the $\boldsymbol{ab}$ plane was detected by ^{51}V NMR. In both the HTI and the LTI phases two prominent spin components of the Ni_s spins $S_a \approx S_c \gg S_b$ are revealed at magnetic field below 4.7 T. The phase relationship existing between spin components in the LTI phase cannot be determined unambiguously from the NMR data measured at rather high magnetic fields approaching the first-order LTI—C phase transition at $\boldsymbol{H} \| \boldsymbol{c}$. One needs NMR data measured at lower magnetic field to clear up the SDW polarization in the LTI phase. (d) The macroscopic magnetization of NVO can be explained due to the uniform polarization of the antiferromagnetic structure of the Ni_c spins canted along magnetic field.

ACKNOWLEDGMENTS

This work was supported in part by the Russian Foundation for Basic Research (Grants No. 08-02-00029a and No. 09-02-00310a) and the Belarusian State Fund for Fundamental Research (Grants No. F08R-177 and No. F09K-017). V.O. and A.Y. are grateful to the administration staff of the Hokkaido University for hospitality and support.

[1] N. Rogado, M. Haas, G. Lawes, D. A. Huse, A. Ramirez, and R. Cava, J. Phys.: Condens. Matter **15**, 907 (2003).
[2] N. Rogado, G. Lawes, D. Huse, A. Ramirez, and R. Cava, Solid State Commun. **124**, 229 (2002).
[3] G. Lawes *et al.*, Phys. Rev. Lett. **93**, 247201 (2004).
[4] G. Lawes *et al.*, Phys. Rev. Lett. **95**, 087205 (2005).
[5] M. Kenzelmann, A. B. Harris, S. Jonas, C. Broholm, J. Schefer, S. B. Kim, C. L. Zhang, S.-W. Cheong, O. P. Vajk, and J. W. Lynn, Phys. Rev. Lett. **95**, 087206 (2005).
[6] A. B. Harris, Phys. Rev. B **76**, 054447 (2007).
[7] A. Harris and G. Lawes, arXiv:cond-mat/0508617 (unpublished).
[8] M. Mostovoy, Phys. Rev. Lett. **96**, 067601 (2006).
[9] R. C. Rai, J. Cao, S. Brown, J. L. Musfeldt, D. Kasinathan, D. J. Singh, G. Lawes, N. Rogado, R. J. Cava, and X. Wei, Phys. Rev. B **74**, 235101 (2006).
[10] E. Sauerbrei, R. Faggiani, and C. Calvo, Acta Crystallogr., Sect. B: Struct. Crystallogr. Cryst. Chem. **29**, 2304 (1973).
[11] M. Kenzelmann *et al.*, Phys. Rev. B **74**, 014429 (2006).
[12] B. Pahari, K. Ghoshray, R. Sarkar, B. Bandyopadhyay, and A. Ghoshray, Phys. Rev. B **73**, 012407 (2006).
[13] V. Ivanov, A. Muhin, A. Kuz'menko, A. Prohorov, A. Pronin, S. Barillo, G. Bychkov, and S. Shiryaev, in *Proceedings of the 11th International Meeting "Order, Disorder and Properties of Oxides*," Rostov-on-Don, Russia (Rostov State University, Rostov-on-Don, 2008), p. 16.
[14] H. Alloul and C. Froidevaux, Phys. Rev. **163**, 324 (1967).
[15] H. Abe, H. Yasuoka, and A. Hirai, J. Phys. Soc. Jpn. **21**, 77 (1966).
[16] Evidently the natural pathway for the *s*-wave spin polarization transfer from Ni to V should include the orbitals, which symmetry is similar to one of the *sp*3-hybridized LCAO, $4s(V)[2p(O)]^3$, providing chemical bonding inside VO_4 tetrahedra.
[17] A. Clogston, A. Gossard, V. Jaccarino, and Y. Yafet, Rev. Mod. Phys. **36**, 170 (1964).
[18] E. Turov and M. Petrov, *Nuclear Magnetic Resonance in Ferro- and Antiferromagnets* (Halsded Press, New York, 1972), p. 207.
[19] F. Borsa and A. Rigamonti, *in Magnetic Resonance of Phase Transitions*, edited by F. J. Owens, Ch. P. Poole, Jr., and H. A. Farach (Academic Press, New York, San Francisco, London, 1979), p. 79.
[20] R. Blinc, Phys. Rep. **79**, 331 (1981).